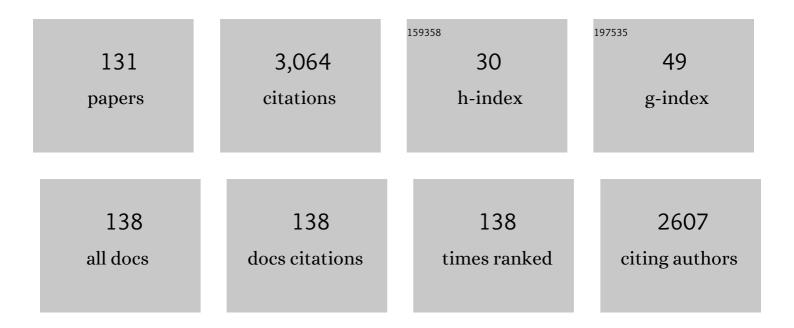
Douglas R. Schmitt

List of Publications by Year in descending order

Source: https://exaly.com/author-pdf/918862/publications.pdf Version: 2024-02-01



#	Article	IF	CITATIONS
1	Simulated annealing inversion of multimode Rayleigh wave dispersion curves for geological structure. Geophysical Journal International, 2002, 151, 622-631.	1.0	224
2	The formation of peak rings in large impact craters. Science, 2016, 354, 878-882.	6.0	181
3	Crustal stress determination from boreholes and rock cores: Fundamental principles. Tectonophysics, 2012, 580, 1-26.	0.9	149
4	Firstâ€break timing: Arrival onset times by direct correlation. Geophysics, 1999, 64, 1492-1501.	1.4	96
5	Repeatability of multimode Rayleighâ€wave dispersion studies. Geophysics, 2003, 68, 782-790.	1.4	84
6	Extreme hydrothermal conditions at an active plate-bounding fault. Nature, 2017, 546, 137-140.	13.7	84
7	Physical properties and seismic imaging of massive sulfides. Geophysics, 2000, 65, 1882-1889.	1.4	76
8	Seismic attributes for monitoring of a shallow heated heavy oil reservoir: A case study. Geophysics, 1999, 64, 368-377.	1.4	72
9	Amplitude and AVO responses of a single thin bed. Geophysics, 2003, 68, 1161-1168.	1.4	71
10	Diminished pore pressure in lowâ€porosity crystalline rock under tensional failure: Apparent strengthening by dilatancy. Journal of Geophysical Research, 1992, 97, 273-288.	3.3	67
11	A revised crustal stress orientation database for Canada. Tectonophysics, 2014, 636, 111-124.	0.9	65
12	A comparative study of the anisotropic dynamic and static elastic moduli of unconventional reservoir shales: Implication for geomechanical investigations. Geophysics, 2016, 81, D245-D261.	1.4	65
13	Measurement of total porosity for gas shales by gas injection porosimetry (GIP) method. Fuel, 2016, 186, 694-707.	3.4	60
14	Drilling-induced core fractures and in situ stress. Journal of Geophysical Research, 1998, 103, 5225-5239.	3.3	55
15	Inherent transversely isotropic elastic parameters of over-consolidated shale measured by ultrasonic waves and their comparison with static and acoustic <i>in situ</i> log measurements. Journal of Geophysics and Engineering, 2008, 5, 103-117.	0.7	55
16	Intrinsic elasticity of a textured transversely isotropic muscovite aggregate: Comparisons to the seismic anisotropy of schists and shales. Journal of Geophysical Research, 2006, 111, .	3.3	52
17	Shock temperatures in silica glass: Implications for modes of shockâ€induced deformation, phase transformation, and melting with pressure. Journal of Geophysical Research, 1989, 94, 5851-5871.	3.3	51
18	Compressionalâ€wave velocities in attenuating media: A laboratory physical model study. Geophysics, 2000, 65, 1162-1167.	1.4	49

#	Article	IF	CITATIONS
19	Mapping fractures with GPR: A case study from Turtle Mountain. Geophysics, 2006, 71, B139-B150.	1.4	49
20	Measurement of the speed and attenuation of the Biot slow wave using a large ultrasonic transmitter. Journal of Geophysical Research, 2009, 114, .	3.3	49
21	Static and dynamic pressure sensitivity anisotropy of a calcareous shale. Geophysical Prospecting, 2016, 64, 875-897.	1.0	49
22	Quantitative constraints to the complete state of stress from the combined borehole and focal mechanism inversions: Fox Creek, Alberta. Tectonophysics, 2019, 764, 110-123.	0.9	44
23	CO2 rock physics as part of the Weyburn-Midale geological storage project. International Journal of Greenhouse Gas Control, 2013, 16, S118-S133.	2.3	39
24	Measuring velocity dispersion and attenuation in the exploration seismic frequency band. Geophysics, 2009, 74, WA113-WA122.	1.4	37
25	Experimental determination of the elastic coefficients of an orthorhombic material. Geophysics, 2001, 66, 1217-1225.	1.4	35
26	High-resolution seismic and resistivity profiling of a buried Quaternary subglacial valley: Northern Alberta, Canada. Bulletin of the Geological Society of America, 2009, 121, 1570-1583.	1.6	33
27	Laboratory measurements of static and dynamic bulk moduli in carbonate. , 2009, , .		33
28	A versatile facility for laboratory studies of viscoelastic and poroelastic behaviour of rocks. Review of Scientific Instruments, 2011, 82, 064501.	0.6	33
29	Optimization of fringe pattern calculation with direct correlations in speckle interferometry. Applied Optics, 1997, 36, 8848.	2.1	32
30	Determination of the complete elastic stiffnesses from ultrasonic phase velocity measurements. Journal of Geophysical Research, 2003, 108, ECV 6-1-ECV 6-11.	3.3	32
31	The first deep heat flow determination in crystalline basement rocks beneath the Western Canadian Sedimentary Basin. Geophysical Journal International, 2014, 197, 731-747.	1.0	31
32	Petrophysical, Geochemical, and Hydrological Evidence for Extensive Fractureâ€Mediated Fluid and Heat Transport in the Alpine Fault's Hangingâ€Wall Damage Zone. Geochemistry, Geophysics, Geosystems, 2017, 18, 4709-4732.	1.0	31
33	Temperatures of shockâ€induced shear instabilities and their relationship to fusion curves. Geophysical Research Letters, 1983, 10, 1077-1080.	1.5	29
34	Ultrasonic anisotropic phase velocity determination with the Radon transformation. Journal of the Acoustical Society of America, 1997, 101, 3278-3286.	0.5	28
35	Velocity anisotropy observed in wellbore seismic arrivals: Combined effects of intrinsic properties and layering. Geophysics, 1996, 61, 12-20.	1.4	28
36	Neogene tectonic and climatic evolution of the Western Ross Sea, Antarctica — Chronology of events from the AND-1B drill hole. Global and Planetary Change, 2012, 96-97, 189-203.	1.6	27

#	Article	IF	CITATIONS
37	Frictional Stabilities on Induced Earthquake Fault Planes at Fox Creek, Alberta: A Pore Fluid Pressure Dilemma. Geophysical Research Letters, 2019, 46, 8753-8762.	1.5	26
38	Depth migration of deep seismic reflection profiles: crustal thickness variations in Alberta. Canadian Journal of Earth Sciences, 2002, 39, 331-350.	0.6	25
39	Seismic anisotropy in the crystalline upper crust: observations and modelling from the Outokumpu scientific borehole, Finland. Geophysical Journal International, 2012, 189, 541-553.	1.0	24
40	Bedrock geology of DFDP-2B, central Alpine Fault, New Zealand. New Zealand Journal of Geology, and Geophysics, 2017, 60, 497-518.	1.0	24
41	Flin Flon Belt seismic anisotropy: elastic symmetry, heterogeneity, and shear-wave splitting. Canadian Journal of Earth Sciences, 2005, 42, 533-554.	0.6	23
42	The Transition Between the Scale Domains of Ray and Effective Medium Theory and Anisotropy: Numerical Models. Pure and Applied Geophysics, 2006, 163, 1327-1349.	0.8	23
43	Ultrasonic shear wave reflectometry applied to the determination of the shear moduli and viscosity of a viscoelastic bitumen. Fuel, 2018, 232, 506-518.	3.4	23
44	Three-dimensional stress relief displacement resulting from drilling a blind hole in acrylic. Experimental Mechanics, 1996, 36, 412-420.	1.1	22
45	Inversion of speckle interferometer fringes for hole-drilling residual stress determinations. Experimental Mechanics, 2000, 40, 129-137.	1.1	22
46	A large ultrasonic bounded acoustic pulse transducer for acoustic transmission goniometry: Modeling and calibration. Journal of the Acoustical Society of America, 2006, 119, 54-64.	0.5	22
47	Effects of Kerogen Content on Elastic Propertiesâ€Based on Artificial Organicâ€Rich Shale (AORS). Journal of Geophysical Research: Solid Earth, 2019, 124, 12660-12678.	1.4	22
48	Shockâ€induced melting and shear banding in singleâ€crystal NaCl. Journal of Applied Physics, 1988, 63, 99-106.	1.1	21
49	Effects of poisson's ratio and core stub length on bottomhole stress concentrations. International Journal of Rock Mechanics and Minings Sciences, 1997, 34, 761-773.	2.6	21
50	Anisotropic elastic moduli of carbonates and evaporites from the Weyburnâ€Midale reservoir and seal rocks. Geophysical Prospecting, 2013, 61, 363-379.	1.0	20
51	An integrative geothermal resource assessment study for the siliciclastic Granite Wash Unit, northwestern Alberta (Canada). Environmental Earth Sciences, 2014, 72, 4141-4154.	1.3	19
52	Modeling of viscoelastic properties of nonpermeable porous rocks saturated with highly viscous fluid at seismic frequencies at the core scale. Journal of Geophysical Research: Solid Earth, 2017, 122, 6067-6086.	1.4	19
53	Pressure and temperature dependence of acoustic wave speeds in bitumen-saturated carbonates: Implications for seismic monitoring of the Grosmont Formation. Geophysics, 2017, 82, MR133-MR151.	1.4	19
54	First Results from HOTSPOT: The Snake River Plain Scientific Drilling Project, Idaho, U.S.A Scientific Drilling, 0, 15, 36-45.	1.0	19

#	Article	IF	CITATIONS
55	Does wettability influence seismic wave propagation in liquid-saturated porous rocks?. Geophysical Journal International, 2015, 203, 2182-2188.	1.0	18
56	Seismic imaging of massive sulfide deposits; Part III, Borehole seismic imaging of near-vertical structures. Economic Geology, 1996, 91, 835-840.	1.8	17
57	In situ seismic measurements in borehole LBâ€08A in the Bosumtwi impact structure, Ghana: Preliminary interpretation. Meteoritics and Planetary Science, 2007, 42, 755-768.	0.7	17
58	Advanced seismic imaging techniques characterize the Alpine Fault at Whataroa (New Zealand). Journal of Geophysical Research: Solid Earth, 2016, 121, 8792-8812.	1.4	17
59	Effects of space exposure on ion-beam-deposited silicon-carbide and boron-carbide coatings. Applied Optics, 1998, 37, 8038.	2.1	16
60	Mapping the geometry of an aquifer system with a high-resolution reflection seismic profile. Geophysical Prospecting, 2005, 53, 817-828.	1.0	16
61	Quantitative modeling of reflected ultrasonic bounded beams and a new estimate of the Schoch shift. IEEE Transactions on Ultrasonics, Ferroelectrics, and Frequency Control, 2008, 55, 2661-2673.	1.7	15
62	Near point-source longitudinal and transverse mode ultrasonic arrays for material characterization. IEEE Transactions on Ultrasonics, Ferroelectrics, and Frequency Control, 2001, 48, 691-698.	1.7	14
63	Monitoring Results after 36 Ktonnes of Deep CO2 Injection at the Aquistore CO2 Storage Site, Saskatchewan, Canada. Energy Procedia, 2017, 114, 4056-4061.	1.8	14
64	The Alpine Fault Hangingwall Viewed From Within: Structural Analysis of Ultrasonic Image Logs in the DFDPâ€⊋B Borehole, New Zealand. Geochemistry, Geophysics, Geosystems, 2018, 19, 2492-2515.	1.0	14
65	Estimation of δand <i>C</i> ₁₃ of organic-rich shale from laser ultrasonic technique measurement. Geophysics, 2018, 83, C137-C152.	1.4	13
66	Least-squares local Radon transforms for dip-dependent GPR image decomposition. Journal of Applied Geophysics, 2006, 59, 224-235.	0.9	12
67	Seismic refraction traveltime inversion for static corrections in a glaciated shield rock environment: a case study. Geophysical Prospecting, 2009, 57, 997-1008.	1.0	12
68	Acoustic Reflectivity From Variously Oriented Orthorhombic Media: Analogies to Seismic Responses From a Fractured Anisotropic Crust. Journal of Geophysical Research: Solid Earth, 2017, 122, 10,069.	1.4	12
69	Seismic rock physics of steam injection in bituminous oil reservoirs. The Leading Edge, 2008, 27, 1132-1137.	0.4	11
70	A Broadband Laboratory Study of the Seismic Properties of Cracked and Fluid‧aturated Synthetic Glass Media. Journal of Geophysical Research: Solid Earth, 2018, 123, 3501-3538.	1.4	11
71	States of In Situ Stress in the Duvernay East Shale Basin and Willesden Green of Alberta, Canada: Variable In Situ Stress States Effect Fault Stability. Journal of Geophysical Research: Solid Earth, 2021, 126, e2020JB021221.	1.4	11
72	Subsurface Tunnel Detection Using Electrical Resistivity Tomography and Seismic Refraction Tomography: A Case Study. , 2010, , .		11

#	Article	IF	CITATIONS
73	Elastic Anisotropy of a Metamorphic Rock Sample of the Canadian Shield in Northeastern Alberta. Rock Mechanics and Rock Engineering, 2015, 48, 1369-1385.	2.6	10
74	The longitudinal modulus of bitumen: Pressure and temperature dependencies. Geophysics, 2019, 84, MR139-MR151.	1.4	10
75	Effective Stress Coefficient for Seismic Velocities in Carbonate Rocks: Effects of Pore Characteristics and Fluid Types. Pure and Applied Geophysics, 2019, 176, 1467-1485.	0.8	10
76	Broadband laboratory measurements of dispersion in thermally cracked and fluid-saturated quartzite and a synthetic analogue. The Leading Edge, 2014, 33, 624-632.	0.4	9
77	A program to calculate pulse transmission responses through transversely isotropic media. Computers and Geosciences, 2018, 114, 59-72.	2.0	9
78	A program to calculate the state of stress in the vicinity of an inclined borehole through an anisotropic rock formation. Geophysics, 2019, 84, F103-F118.	1.4	9
79	Inâ€situ holographic elastic moduli measurements from boreholes. Geophysics, 1989, 54, 468-477.	1.4	8
80	Point load determination of static elastic moduli using laser speckle interferometry. Optics and Lasers in Engineering, 2004, 42, 511-527.	2.0	8
81	Shear Modulus Dispersion in Cracked and Fluidâ€Saturated Quartzites: Experimental Observations and Modeling. Journal of Geophysical Research: Solid Earth, 2018, 123, 2825-2840.	1.4	8
82	Fracture Statistics Derived From Digital Ultrasonic Televiewer Logging. Journal of Canadian Petroleum Technology, 1993, 32, .	2.3	7
83	A high-pressure technique for determining the microcrack porosities of damaged brittle materials. Canadian Journal of Physics, 1995, 73, 330-337.	0.4	7
84	Three-dimensional stress-relief displacements from blind-hole drilling: a parametric description. Experimental Mechanics, 2003, 43, 52-60.	1.1	7
85	Acoustic reflectivity goniometry of bounded ultrasonic pulses: Experimental verification of numerical models. Journal of Applied Physics, 2008, 104, 064914.	1.1	7
86	Seismic Measurements for Detecting Underground Highâ€Contrast Voids. , 2009, , .		7
87	Quantitative determination of stress by inversion of speckle interferometer fringe patterns: experimental laboratory tests. Geophysical Journal International, 2006, 167, 1425-1438.	1.0	6
88	Initial seismic observations from a deep borehole drilled into the Canadian Shield in northeast Alberta. International Journal of Earth Sciences, 2015, 104, 1549-1562.	0.9	6
89	The Bow City structure, southern Alberta, Canada: The deep roots of a complex impact structure?. Meteoritics and Planetary Science, 2014, 49, 872-895.	0.7	5
90	Detailed topography of the Devonian Grosmont Formation surface from legacy high-resolution seismic profiles, northeast Alberta. Geophysics, 2014, 79, B135-B149.	1.4	5

#	Article	IF	CITATIONS
91	ARTc: Anisotropic reflectivity and transmissivity calculator. Computers and Geosciences, 2016, 93, 114-126.	2.0	5
92	Accounting for pressure-dependent ultrasonic beam skew in transversely isotropic rocks: combining modelling and measurement of anisotropic wave speeds. Geophysical Journal International, 2020, 221, 231-250.	1.0	5
93	A program to forward model the failure pattern around the wellbore in elastic and strength anisotropic rock formations. International Journal of Rock Mechanics and Minings Sciences, 2022, 151, 105035.	2.6	5
94	Applications of real time digital acquisition of ultrasonic borehole televiewer data on a personal computer. Review of Scientific Instruments, 1992, 63, 3767-3772.	0.6	4
95	Effects of Explosives on Incubating Lake Trout Eggs in the Canadian Arctic. North American Journal of Fisheries Management, 2006, 26, 833-842.	0.5	4
96	Effects of Simulated Blasting on Mortality of Rainbow Trout Eggs. Transactions of the American Fisheries Society, 2008, 137, 1-12.	0.6	4
97	1. Heavy-Oil Reservoirs: Their Characterization and Production. , 2010, , 1-69.		4
98	Geothermal energy potential of sedimentary formations in the Athabasca region, northeast Alberta, Canada. Interpretation, 2016, 4, SR19-SR33.	0.5	4
99	Geophysical evidence for an igneous dike swarm, Buffalo Creek, Northeast Alberta. Bulletin of the Geological Society of America, 2018, 130, 1059-1072.	1.6	4
100	Seismic <i>P</i> ÂWave Velocity Model From 3â€D Surface and Borehole Seismic Data at the Alpine Fault DFDPâ€2 Drill Site (Whataroa, New Zealand). Journal of Geophysical Research: Solid Earth, 2020, 125, e2019JB018519.	1.4	4
101	22. Integrating Seismic-Velocity Tomograms and Seismic Imaging: Application to the Study of a Buried Valley. , 2010, , 361-378.		4
102	Intensity and Position Measuring Systems in the Booster of the Zero Gradient Synchrotron. IEEE Transactions on Nuclear Science, 1977, 24, 1739-1741.	1.2	3
103	Model-based inversion of speckle interferometer fringe patterns. Applied Optics, 1998, 37, 2573.	2.1	3
104	Modelling the effect of seismic velocity gradients on the change in geometrical spreading across a boundary. Geophysical Journal International, 2001, 146, 679-690.	1.0	3
105	Seismic imaging through the volcanic rocks of the Snake River Plain: insights from Project Hotspot. Geophysical Prospecting, 2015, 63, 919-936.	1.0	3
106	Laboratory determination of elastic anisotropy in shales from Alberta. , 2006, , .		3
107	Pole Face Winding (PFW) Equipment for Eddy Current Correction at the Zero Gradient Synchrotron (ZGS). IEEE Transactions on Nuclear Science, 1973, 20, 397-398.	1.2	2
108	Time-lapse speckle interferometry. Geophysical Research Letters, 1999, 26, 2589-2592.	1.5	2

#	Article	IF	CITATIONS
109	Sensitivity of seismic response for monitoring storage in a low porosity reservoir of the St Lawrence Lowlands, Québec, Canada: Part 2 – Synthetic modeling. , 2017, 7, 613-623.		2
110	Plain Language Summary Required for Submission to Journal of Geophysical Research: Solid Earth. Journal of Geophysical Research: Solid Earth, 2021, 126, e2021JB022351.	1.4	2
111	6. Seismic Rock Physics of Steam Injection in Bituminous-Oil Reservoirs. , 2010, , 107-112.		2
112	A Review of Methods for Estimating Ballast Degradation Using Ground-Penetrating Radar. , 2018, , 54-76.		2
113	3D active source seismic imaging of the Alpine Fault zone and the Whataroa glacial valley in New Zealand. Journal of Geophysical Research: Solid Earth, 0, , .	1.4	2
114	Active and Passive Seismic as an Indicator of Large Equipment Interactions with the Oil Sand. Geotechnical and Geological Engineering, 2010, 28, 727-743.	0.8	1
115	An algorithm for quantitatively modeling reflected ultrasonic bounded pulses and beams. Ultrasonics, 2017, 80, 15-21.	2.1	1
116	Sensitivity of seismic response for monitoring storage in a low porosity reservoir of the St Lawrence Lowlands, Québec, Canada: Part 1 – Laboratory measurements. , 2017, 7, 602-612.		1
117	Always finding faults: New Zealand 2016. , 2017, , .		1
118	The spatial correlation between track roughness and ground-penetrating radar inferred ballast degradation. Proceedings of the Institution of Mechanical Engineers, Part F: Journal of Rail and Rapid Transit, 2018, 232, 1917-1931.	1.3	1
119	Evaluating the sensitivity of low-frequency ground-penetrating radar attributes to estimate ballast fines in the presence of variable track foundations through simulation. Proceedings of the Institution of Mechanical Engineers, Part F: Journal of Rail and Rapid Transit, 2018, 232, 1168-1181.	1.3	1
120	Shallow seismic reflection imaging of the Alpine Fault through late Quaternary sedimentary units at Whataroa, New Zealand. New Zealand Journal of Geology, and Geophysics, 2021, 64, 505-517.	1.0	1
121	Empirical rock physics relationships on carbonate dry-frame elastic properties. Petroleum Science, 2021, 18, 783.	2.4	1
122	Analysis of 4D time-lapse seismic responses integrated with 3D data products, production information, and laboratory data to characterize a bitumen-bearing carbonate reservoir. , 2016, , .		1
123	Borehole Seismic Observations From the Chicxulub Impact Drilling: Implications for Seismic Reflectivity and Impact Damage. Geochemistry, Geophysics, Geosystems, 2022, 23, .	1.0	1
124	High resolution seismic imaging of a shallow gas reservoir, Alberta, Canada. , 2006, , .		0
125	Laboratory experiments and numerical simulation on Bitumen Saturated Carbonates: A Rock Physics Study for 4D Seismology. ASEG Extended Abstracts, 2016, 2016, 1-5.	0.1	0
126	Thank You to Our 2018 Peer Reviewers. Journal of Geophysical Research: Solid Earth, 2019, 124, 3242-3253.	1.4	0

#	Article	IF	CITATIONS
127	Thank You to Our 2019 Reviewers. Journal of Geophysical Research: Solid Earth, 2020, 125, e2020JB019781.	1.4	Ο
128	Thank You to Our 2020 Peer Reviewers. Journal of Geophysical Research: Solid Earth, 2021, 126, e2021JB021896.	1.4	0
129	Application of Local Radon Transforms for dipâ \in dependent GPR image decomposition. , 2005, , .		0
130	20. Collaborative Methods in Enhanced Cold Heavy-Oil Production. , 2010, , 251-257.		0
131	Thank You to Our 2021 Peer Reviewers. Journal of Geophysical Research: Solid Earth, 0, , .	1.4	0